

## Controlled Self-Assembly of Carbohydrate Conjugate Rod–Coil Amphiphiles for Supramolecular Multivalent Ligands

Byung-Sun Kim, Dong-Je Hong, Jinyoung Bae, and Myongsoo Lee\*

Contribution from the Center for Supramolecular Nano-Assembly and Department of Chemistry, Yonsei University, Seoul 120-749, Korea

Received August 31, 2005; E-mail: mslee@yonsei.ac.kr

**Abstract:** Carbohydrate conjugate rod–coil amphiphiles were synthesized and their self-assembling behavior in aqueous solution was investigated. These amphiphiles were observed to self-assemble into supramolecular structures that differ significantly depending on the molecular architecture. The rod–coil amphiphiles based on a short coil (**1**) self-assemble into a vesicular structure, while the amphiphiles with a long coil (**2**) show a spherical micellar structure. In contrast, **3**, based on a twin-rod segment, was observed to aggregate into cylindrical micelles with twice the diameter of molecular length scale. As a means to determine the binding activity to protein receptors of these supramolecular objects, hemagglutination inhibition assay was performed. The experiments showed that the supramolecular architecture has a significant effect on the binding activity. In addition, incubation experiments with *Escherichia coli* showed that mannose-coated objects specifically bind to the bacterial pili of the ORN 178 strain. These results demonstrate that precise control of the nano-objects in shape and size by molecular design can provide control of the biological activities of the supramolecular materials.

### Introduction

Novel approaches to the development of artificial multivalent carbohydrate conjugate objects remain important area of research due to their strong and specific interactions with the receptor proteins.<sup>1</sup> Many different designs of multivalent ligands have been reported, with a number of scaffolds including glycoproteins,<sup>2</sup> linear polymers,<sup>3</sup> and dendrimers.<sup>4</sup> Alternatively, self-assembly of amphiphilic molecules containing carbohydrate moieties is known to play a role in efficient multivalent ligands.<sup>5</sup> The self-assembly of incompatible molecular components leading to microphase separation comprises a powerful approach toward the fabrication of complex nanoarchitectures and plays an essential role in living systems, for example, in protein

folding and the formation of biological membranes.<sup>6</sup> Extensive efforts thus have been directed toward bioactive supramolecular systems for exploration of novel properties and functions that are difficult without specific assembly of molecular components.<sup>7</sup> Block molecules that mimic lipid amphiphilicity have been proved to be promising scaffolds for nanometer-sized aggregates with well-defined size and shape.<sup>8</sup> Introduction of a rigid segment into a self-assembling system has been reported to enhance aggregation stability.<sup>9</sup> In addition to stability, another important issue regarding the preparation of nanometer-scale aggregates is their capability to interact with biological receptors.<sup>10</sup> To obtain precisely controlled and well-defined aggregates with biological functions, however, the more elaborate design of corresponding building blocks bearing bioactive moieties is

- (1) (a) Lundquist, J. J.; Toone, E. J. *Chem. Rev.* **2002**, *102*, 555–578. (b) Gestwicki, J. E.; Cario, C. W.; Strong, L. E.; Oetjen, K. A.; Kiessling, L. L. *J. Am. Chem. Soc.* **2002**, *124*, 14922–14933. (c) Mammen, M.; Choi, S.-K.; Whitesides, G. M. *Angew. Chem., Int. Ed.* **1998**, *37*, 2754–2794.
- (2) Bertozzi, C. R.; Kiessling, L. L. *Science* **2001**, *291*, 2357–2364.
- (3) (a) Disney, M. D.; Zheng, J.; Swager, T. M.; Seeburger, P. H. *J. Am. Chem. Soc.* **2004**, *126*, 13343–13346. (b) Kim, I.-B.; Wilson, J. N.; Bunz, U. H. F. *Chem. Commun.* **2005**, 1273–1275. (c) Gestwicki, J. E.; Kiessling, L. L. *Nature* **2002**, *415*, 81–84. (d) Sasaki, K.; Nishida, Y.; Tsurumi, T.; Uzawa, H.; Kondo, H.; Kobayashi, K. *Angew. Chem., Int. Ed.* **2002**, *41*, 4463–4467. (e) Cario, C. W.; Gestwicki, J. E.; Kanai, M.; Kiessling, L. L. *J. Am. Chem. Soc.* **2002**, *124*, 1615–1619.
- (4) (a) Woller, E. K.; Walter, E. D.; Morgan, J. R.; Singel, D. J.; Cloninger, M. J. *J. Am. Chem. Soc.* **2003**, *125*, 8820–8826. (b) Roy, R.; Kim, J. M. *Angew. Chem., Int. Ed.* **1998**, *38*, 369–372. (c) Baussanne, I.; Law, H.; Defaye, J.; Benito, J. M.; Mellet, C. O.; Fernandez, J. M. G. *Chem. Commun.* **2000**, 1489–1490.
- (5) (a) Thoma, G.; Katopodis, A. G.; Voelcker, N.; Duthaler, R. O.; Streiff, M. B. *Angew. Chem., Int. Ed.* **2002**, *41*, 3195–3198. (b) Aoyama, Y.; Kanamori, T.; Nakai, T.; Sasaki, T.; Horiuchi, S.; Sando, S.; Niidome, T. *J. Am. Chem. Soc.* **2003**, *125*, 3455–3457. (c) de la Fuente, J. M.; Barrientos, A. G.; Rojas, T. C.; Rojo, J.; Cañada, J.; Fernández, A.; Penadés, S. *Angew. Chem., Int. Ed.* **2001**, *40*, 2258–2261. (d) Lin, C.-C.; Yeh, Y.-C.; Yang, C.-Y.; Chen, C.-L.; Chen, G.-F.; Chen, C.-C.; Wu, Y.-C. *J. Am. Chem. Soc.* **2002**, *124*, 3508–3509.
- (6) (a) Wong, G. C. L.; Tang, J. X.; Lin, A.; Li, Y.; Janmey, P. A.; Safinya, C. R. *Science* **2000**, *288*, 2035–2039. (b) Elemans, J. A. A. W.; Rowan, A. E.; Nolte, R. J. M. *J. Mater. Chem.* **2003**, *13*, 2661–2670. (c) Hartgerink, J. D.; Beniash, E.; Stupp, S. I. *Science* **2001**, *294*, 1684–1687.
- (7) (a) Ooya, T.; Utsunomiya, H.; Eguchi, M.; Yui, N. *Bioconjugate Chem.* **2005**, *16*, 62–69. (b) Haag, R. *Angew. Chem., Int. Ed.* **2004**, *43*, 278–282. (c) Savic, R.; Luo, L.; Eisenberg, A.; Maysinger, D. *Science* **2003**, *300*, 615–618. (d) Aggeli, A.; Bell, M.; Carrick, L. M.; Fichwick, C. W. G.; Harding, R.; Mawer, P. J.; Radford, S. E.; Strong, A. E.; Boden, N. *J. Am. Chem. Soc.* **2003**, *125*, 9619–9628.
- (8) (a) Förster, S.; Konrad, M. *J. Mater. Chem.* **2003**, *13*, 2671–2688. (b) Lee, M.; Cho, B.-K.; Zin, W.-C. *Chem. Rev.* **2001**, *101*, 3869–3892.
- (9) (a) Yoo, Y.-S.; Choi, J.-H.; Song, J.-H.; Oh, N.-K.; Zin, W.-C.; Park, S.; Chang, T.; Lee, M. *J. Am. Chem. Soc.* **2004**, *126*, 6294–6300. (b) Jang, C.-J.; Ryu, J.-H.; Lee, J.-D.; Sohn, D.; Lee, M. *Chem. Mater.* **2004**, *16*, 4226–4231. (c) Vriezema, D. M.; Hoogboom, J.; Velonia, K.; Takazawa, K.; Christianen, P. C. M.; Maan, J. C.; Rowan, A. E.; Nolte, R. J. M. *Angew. Chem., Int. Ed.* **2003**, *42*, 772–776. (d) Kukula, H.; Schlaad, H.; Antonietti, M.; Förster, S. *J. Am. Chem. Soc.* **2002**, *124*, 1658–1663. (e) Chécot, F.; Lecommandoux, S.; Gnanou, Y.; Klok, H.-A. *Angew. Chem., Int. Ed.* **2002**, *41*, 1340–1343.
- (10) Kim, B.-S.; Yang, W.-Y.; Ryu, J.-H.; Yoo, Y.-S.; Lee, M. *Chem. Commun.* **2005**, 2035–2037.

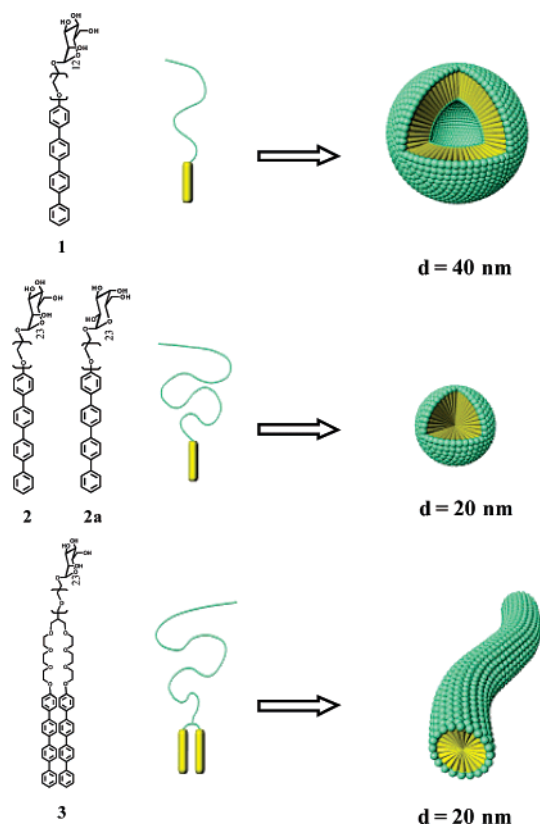


**Figure 1.** Molecular structure of **1–3** and schematic representation of vesicles and spherical and cylindrical micelles.

required, since the information determining their specific assembly should be encoded in their molecular architecture. Accordingly, we synthesized rod–coil amphiphiles bearing carbohydrates at one end of the coil segment that can endow aggregates with enhanced stability and biological functions. In this paper, we report significant size and structural changes of the carbohydrate-coated aggregates, from vesicles to cylindrical micelles to spherical micelles, with only small variations in molecular architecture of the rod–coil amphiphiles **1–3** (Figure 1). These aggregates were observed to function as multivalent ligands in the presence of natural receptors.

## Results and Discussion

The amphiphilic rod–coil molecules consisting of tetra(*p*-phenylene) or di[tetra(*p*-phenylene)] as a rod segment and  $\alpha$ -D-mannopyranoside-functionalized oligo(ethylene oxide)s as a coil segment were obtained in a multiple synthesis from commercially available starting materials.<sup>10,11</sup> For comparison, the homologous amphiphile of **2** bearing  $\beta$ -D-galactopyranoside (**2a**) instead of  $\alpha$ -D-mannopyranoside was also synthesized and characterized. The resulting rod–coil amphiphiles were characterized by <sup>1</sup>H and <sup>13</sup>C NMR spectroscopy, elemental analysis, and matrix-assisted laser desorption ionization time-of-flight (MALDI-TOF) mass spectroscopy and were shown to be in full agreement with the structures presented.

All of the molecules in aqueous solution showed an aggregation behavior with a relatively narrow size distribution, indicating well-equilibrated structures (Figure 2).<sup>12</sup> Previously, dynamic

light scattering (DLS) and transmission electron microscopy (TEM) studies demonstrated that **1** self-assembles into a  $\alpha$ -D-mannopyranoside-coated vesicular structure with an average diameter of approximately 40 nm.<sup>10</sup> Compound **2**, based on a long oligo(ethylene oxide) chain, was also observed to assemble into  $\alpha$ -D-mannopyranoside-coated spherical aggregates, but they are smaller in size. DLS measurements of **2** showed that  $R_H$  is approximately 12 nm with a narrow size distribution. TEM micrographs showed spherical aggregates that are roughly 18–22 nm in diameter and are thus in accord with the DLS results (Figure 3b). These dimensions in diameter of the aggregates, however, correspond to approximately twice the extended molecular length (10 nm by CPK modeling), implying that the aggregates of **2** are micellar in nature. The formation of very small aggregates of higher curvature could be the result of a more cone-shaped conformation of the long chain-based rod–coil molecules compared to **1**. It has been predicted that the self-assembly process is governed by geometrical constraints of individual molecules.<sup>13</sup> As expected, **2a** based on a  $\beta$ -D-galactopyranoside moiety also formed essentially the same spherical micellar objects as those of **2**.

In contrast, compound **3**, based on a twin-rod segment, was observed to aggregate into cylindrical micelles with twice the diameter of molecular length scale. Dynamic light scattering (DLS) experiments were performed with **3** in aqueous solution ( $2 \times 10^{-4}$  g/mL) in order to investigate this unique aggregation behavior (Figure 2). CONTIN analysis of the autocorrelation function shows a broad peak corresponding to an average hydrodynamic radius of approximately 70 nm. The angular dependence of the apparent diffusion coefficient ( $D_{app}$ ) was measured because the slope is related to the shape of the diffusing species.<sup>14</sup> The slope was observed to be 0.03, consistent with the value predicted for cylindrical micelles. The formation of cylindrical micelles was further confirmed by a Kratky plot that shows a linear angular dependence over the scattering light intensity of the aggregates.<sup>15</sup> TEM micrographs of **3** clearly show cylindrical aggregates with a uniform diameter of about 20 nm and lengths up to several micrometers (Figure 3c). Considering the extended molecular length (11 nm by CPK modeling), the image indicates that the diameter of the cylindrical objects corresponds to approximately twice the extended molecular length. All of these data indicate that **3** self-assembles into a cylindrical micellar structure consisting of aromatic cores surrounded by  $\alpha$ -D-mannopyranoside-functionalized coil segments. The cylindrical structure of this micelle might be partly explained by the more tapered shape of individual molecules, compared to **2**, but a second driving force might be strong  $\pi$ – $\pi$  interactions among aromatic segments down the long axis of the cylinders.<sup>16</sup>

Self-assembly of the rod–coil amphiphiles into supramolecular objects coated by carbohydrates suggests that they may

(11) (a) Lee, M.; Jang, C.-J.; Ryu, J.-H. *J. Am. Chem. Soc.* **2004**, *126*, 8082–8083. (b) Lee, M.; Park, M.-H.; Oh, N.-K.; Zin, W.-C.; Jung, H.-T.; Yoon, D. K. *Angew. Chem., Int. Ed.* **2004**, *43*, 6466–6468.

(12) The critical micelle concentrations (cmc) of the molecules, determined by plotting the absorption intensity of a hydrophobic dye, Nile Red, in an aqueous phase against amphiphile concentration, were  $2.3 \times 10^{-6}$  M,  $5.1 \times 10^{-6}$  M, and  $4.8 \times 10^{-7}$  M for **1**, **2**, and **3**, respectively.  
 (13) Israelachvili, J. N. *Intermolecular and Surface Forces*; Academic Press: London, 1992.  
 (14) Gohy, J.-F.; Lohmeijer, B. G. G.; Alexeev, A.; Wang, X.-S.; Manners, I.; Winnik, M. A.; Schubert, U. S. *Chem. Eur. J.* **2004**, *10*, 4315–4323.  
 (15) Bockstaller, M.; Köhler, W.; Wegner, G.; Vlassopoulos, D.; Fytas, G. *Macromolecules* **2000**, *33*, 3951–3953.  
 (16) (a) Percec, V.; Cho, W.-D.; Ungar, G. *J. Am. Chem. Soc.* **2000**, *122*, 10273–10281. (b) Hoeben, F. J. M.; Jonkheijm, P.; Meijer, E. W.; Schenning, A. P. H. *J. Chem. Rev.* **2005**, *105*, 1491–1546.

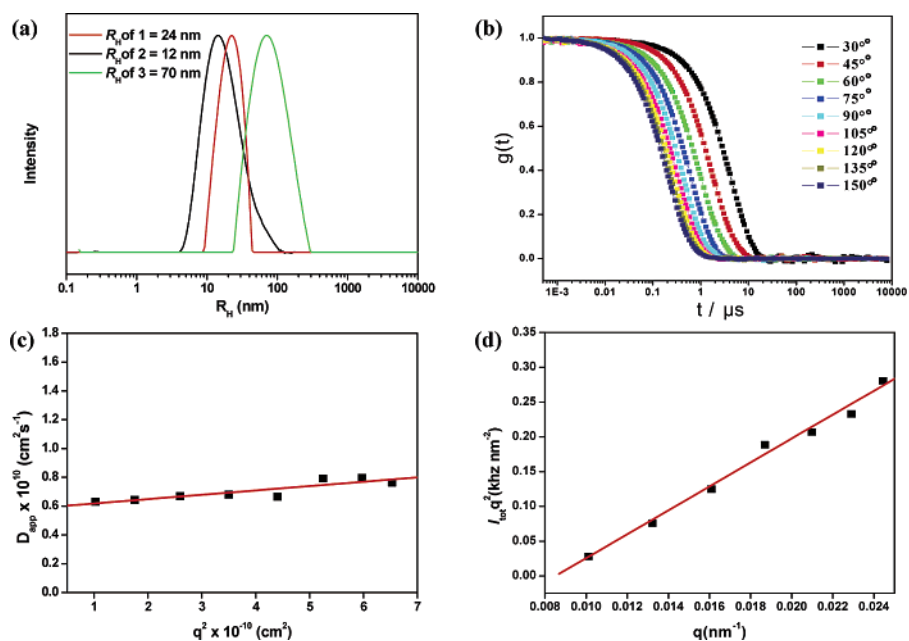


**Figure 2.** (a) Hydrodynamic radius distributions of **1–3**; (b) autocorrelation function of **3**; (c) angular dependence of the diffusion coefficient for **3**; (d) Kratky plot (■) and linear fit of **3** in aqueous solution with concentration of  $2 \times 10^{-4}$  g/mL.

be used as supramolecular multivalent ligands. Toward this direction, hemagglutination inhibition assay with lectin concanavalin A (Con A) was selected because Con A recognizes  $\alpha$ -D-mannopyranoside and these systems have been extensively studied as a model of multivalent interaction.<sup>17–19</sup> The minimum inhibitory concentration (MIC) of  $\alpha$ -D-mannopyranoside unit to inhibit Con A-promoted erythrocyte (rabbit) agglutination was determined for each object. Relative potency was calculated from the ratio of the minimum inhibitory concentrations of the object-bound  $\alpha$ -D-mannopyranoside and methyl mannose as a standard. As shown in Figure 4, all of the objects showed high inhibitory potency in the hemagglutination assay, indicating that multivalent interactions between Con A and  $\alpha$ -D-mannopyranoside units occur. The relative potencies of **1** and **3** showed 800-fold and 1000-fold increases, respectively, over methyl mannose, while **2** showed an 1800-fold increase. These results suggest that the spherical micellar objects with higher curvature are more efficient inhibitors than the vesicular and cylindrical objects. Although the origin of this difference in relative activity depending on the supramolecular objects is not clear at present, the high curvature of the smaller spherical object seems to play an important role in enhanced inhibitory potency.<sup>20,21</sup>

Further information on the Con A–supramolecular object binding events was provided by transmission electron microscopy (TEM) experiments performed at the concentration of the hemagglutination assay (Figure 5). The micrographs of **1**–Con A and **2**–Con A mixtures show spherical aggregates with diameters of 200 and 180 nm, respectively, that are much larger than those of Con A (6.5 nm) and the supramolecular objects (40 and 20 nm for **1** and **2**, respectively), demonstrating that closely packed object–Con A clusters are formed in solution. On the other hand, the micrograph of **3**–Con A mixture shows

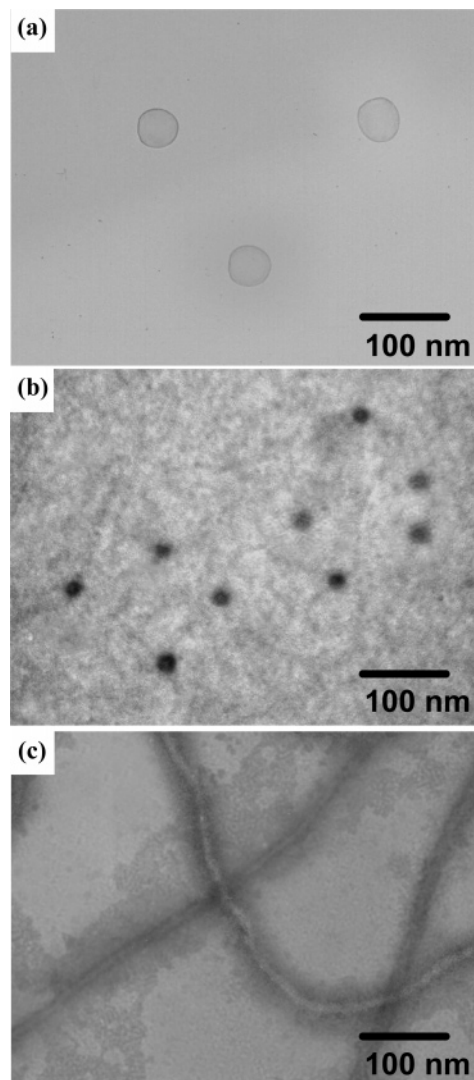


**Figure 3.** TEM images of (a) **1**, (b) **2** without staining, and (c) **3** with negative staining.

(17) Osawa, T.; Matsumoto, I. *Methods Enzymol.* **1972**, *28*, 323–327.

(18) Woller, E. K.; Cloninger, M. J. *Org. Lett.* **2002**, *4*, 7–10.

(19) Strong, L. E.; Kiessling, L. L. *J. Am. Chem. Soc.* **1999**, *121*, 6193–6196.

(20) Lee, R. T.; Lee, Y. C. *Glycoconjugate J.* **2000**, *17*, 543–551.

(21) Schlick, K. H.; Udelhoven, R. A.; Strohmeyer, G. C.; Cloninger, M. J. *Mol. Pharm.* **2005**, *2*, 295–301.

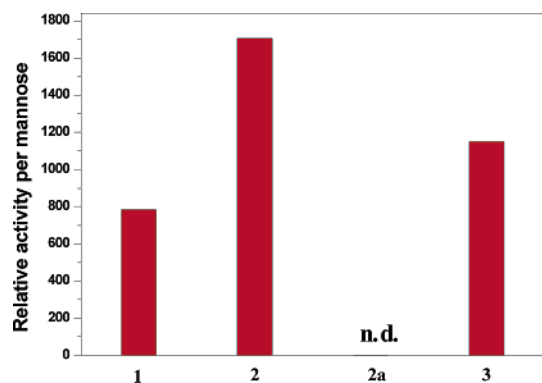


**Figure 4.** Relative activity of Con A-induced hemagglutination inhibition based on the minimum inhibitory concentration (MIC) of **1–3**. (Each value represents at least three experiments; n.d. = not determined.)

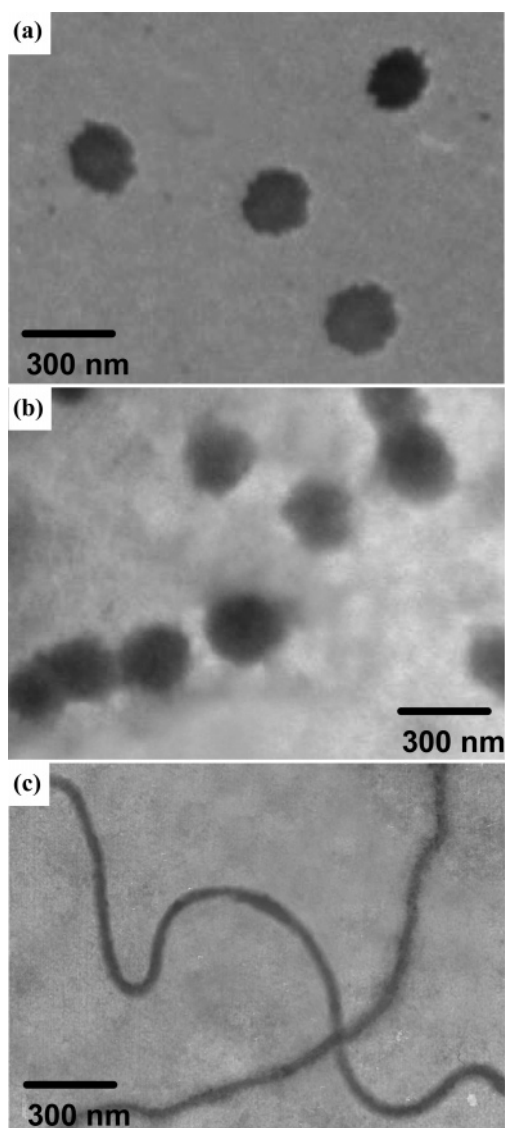


**Figure 5.** TEM images of aqueous solutions of (a) **1** and Con A, (b) **2** and Con A, and (c) **3** and Con A at the hemagglutination inhibition concentration.

cylindrical aggregates with a uniform diameter of 40 nm that is nearly double compared to that of the supramolecular object of **3** (Figure 5c). This result suggests that each cylindrical object is surrounded by lectin proteins through multivalent interactions. The control experiments with  $\beta$ -D-galactopyranoside-coated

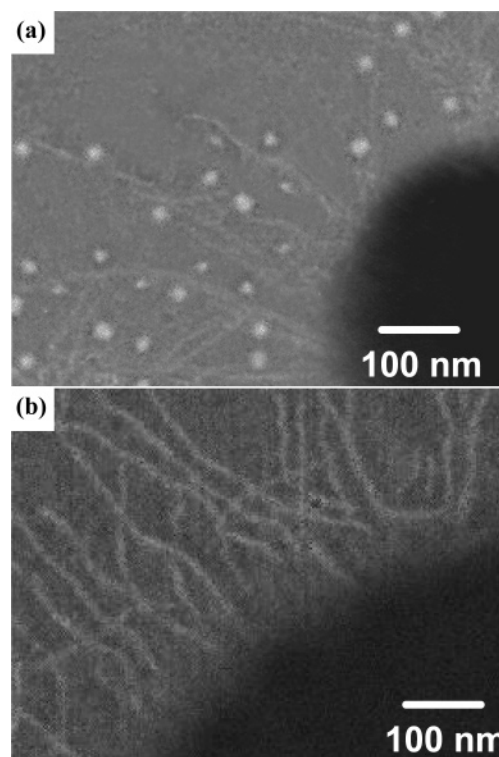


**Figure 6.** TEM images with negative staining of sectioned area of pili of the *E. coli* ORN 178 strain bound with (a) **1** and (b) **2a**. A portion of an *E. coli* is shown in the lower right.

objects of **2a** showed no nonspecific object–Con A association, suggesting that the observed binding activity is specific to the  $\alpha$ -D-mannopyranoside-coated objects.

Interestingly, the micellar objects appeared to specifically bind to FimH adhesin of bacterial type 1 pili in *Escherichia coli*, demonstrating that the objects are excellent multivalent ligands toward the specific receptors on the cell surface. Type 1 pili are heteropolymeric mannose-binding proteinaceous fibers that protrude from the surface of many gram-negative bacterial cells.<sup>22</sup> The bioactive binding ability of the objects was then evaluated by interactions of the spherical micellar object of **2** with bacterial cells via TEM imaging. ORN 178 *E. coli* strain was used in experiments to confirm the binding of the supramolecular objects to FimH.<sup>23</sup> After incubating of the bacterial strain with the objects, the suspensions were centrifuged to pellet the cells that were washed further to remove unbound objects. As shown in Figure 6a, a number of spherical objects were clearly observed to be located along the fibers, indicative of strong binding of the objects to FimH strain. Notably, the shape and size of the objects was retained even after binding to the bacterial pili, indicative of high stability of the supramolecular objects. The strong binding between the objects and FimH seems to be attributed to recognition of multivalent  $\alpha$ -D-mannopyranoside ligands on the surface of a micellar object by the receptors located on the bacterial pili.

This binding event was observed to be specific to the  $\alpha$ -D-mannopyranoside-coated objects. In the control experiments, the

- (22) (a) Jones, C. H.; Pinkner, J. S.; Roth, R.; Heuser, J.; Nicholes, A. V.; Abraham, S. N.; Hultgren, S. J. *Proc. Natl. Acad. Sci. U.S.A.* **1995**, *92*, 2081–2085. (b) Choudhury, D.; Thompson, A.; Stojanoff, V.; Langermann, S.; Pinker, J.; Hultgren, S. J.; Knight, S. D. *Science* **1999**, *285*, 1061–1066.
- (23) Harris, S. L.; Spears, P. A.; Havell, E. A.; Hamrick, T. S.; Horton, J. R.; Orndorff, P. E. *J. Bacteriol.* **2001**, *183*, 4099–4102.

$\beta$ -D-galactopyranoside-coated spherical objects of **2a** were used to replace  $\alpha$ -D-mannopyranoside-coated ones under essentially the same experimental conditions, but no apparent binding was observed (Figure 6b). This suggests that the mannose units located on the micellar surface were responsible for the multivalent binding. To confirm the selective binding to FimH, ORN 208 *E. coli* cells lacking the FimH protein were incubated with the nanocapsules.<sup>23</sup> In contrast to the ORN 178 strain, no supramolecular objects appeared to be imaged through TEM, indicating that the bacterial pili of the ORN 208 strain are unable to mediate  $\alpha$ -D-mannopyranoside selective binding. These results demonstrate that carbohydrate-coated objects designed as multivalent nanoscaffolds for use in selective receptor binding can be constructed from self-assembly of carbohydrate conjugate rod–coil amphiphiles.

### Conclusion

The carbohydrate conjugate rod–coil amphiphiles were synthesized and their self-assembling behavior in aqueous solution was investigated. These amphiphiles were observed to self-assemble into supramolecular structures that differ significantly depending on the molecular architecture. The rod–coil amphiphiles based on a short coil (**1**) self-assemble into a vesicular structure, while the amphiphiles with a long coil (**2**) show a spherical micellar structure. In contrast, compound **3**, based on a twin-rod segment, was observed to aggregate into cylindrical micelles with twice the diameter of molecular length

scale. Consequently, these systems clearly demonstrate the ability to regulate the carbohydrate-coated supramolecular architecture, from vesicular to spherical micellar to cylindrical micellar structures by systematic variation in the length of coil and the number of rods. More important, these objects functioned as supramolecular multivalent ligands for lectin, Con A, and the receptors on *E. coli*. Furthermore, hemagglutination inhibition assay showed that the supramolecular architecture has a significant effect on the binding activity. These results demonstrate that the ability to control and systematically alter the features of supramolecular materials with molecular design can provide novel opportunity to investigate the widespread roles of multivalent binding in biological systems.

**Acknowledgment.** We gratefully acknowledge the National Creative Research Initiative Programs of the Korean Ministry of Science and Technology for financial support of this work. We thank Professor P. E. Orndorff for providing *E. coli* strains and Professor H. S. Kim for hemagglutination assay experiments.

**Supporting Information Available:** Synthetic procedures, characterization, and experimental procedures for hemagglutination inhibition assays (HIA), dynamic light scattering (DLS), and transmission electron microscopy (TEM). This material is available free of charge via the Internet at <http://pubs.acs.org>.

JA055999A